

# Supporting Information

## **Low-dimensional semiconductor superlattices formed by geometric control over nanocrystal attachment: Experimental results**

W. H. Evers, B. Goris, S. Bals, M. Casavola, J. de Graaf, R. van Roij, M. Dijkstra and D.

Vanmaekelbergh

- I Experimental section on synthesis and oriented attachment**
- II Characterization of the shape and the facets of the PbSe nanocrystals by HAADF-STEM**
- III Effect of the crystal size on the attachment of PbSe nanocubes.**
- IV Overview of the structures formed by oriented attachment in a hexane dispersion**
- V Effect of addition of oleic acid capping molecules to the ethylene glycol**
- VI HAADF-STEM study of defects in oriented attachment**
- VII Oriented attachment of PbSe rods and stars**
- VIII Conversion of PbSe sheets to CdSe or  $\text{Cu}_{2-x}\text{Se}$  sheets by ion exchange**
- IX XRD analysis of the structures formed by oriented attachment**
- X GISAXS study of the oriented attachment in the glycol-ethylene/suspension reactor system**

## I Experimental section on synthesis and oriented attachment

*PbSe nanocubes*: PbSe nanocubes were synthesized by a method described by Houtepen *et al*<sup>[1]</sup>. The synthesis was performed in a water and oxygen free environment. (1) 1.9 gram of lead acetate tri hydrate (99.999% Aldrich), 4 mL of diphenyl ether (99% DPE, aldrich), 3 mL of oleic acid (OA, 90% Aldrich) and 16 mL trioctyl phosphine (TOP, 90% Fluka) were heated to 100 °C under low pressure ( $10^{-3}$  bar) for ~3 hours. (2) A second mixture containing 0.31 g Se (99.999% Alfa Aesar) and 4 mL TOP was prepared. Subsequently 11.5 mL of solution (1) and 1.7 ml of solution (2) was injected into 10 mL 190 °C DPE. The reaction mixture was kept at a constant temperature of 145 °C. After 30 seconds to 10 minutes the reaction mixture was quenched with 20 mL butanol and 10 mL methanol. The crude synthesis mixtures were washed twice by precipitating with methanol, centrifugation and redispersion of the sediment in toluene. This resulted in PbSe nanocrystals with a truncated cubic shape, as shown below.

*PbSe stars*: In order to obtain PbSe “stars”, the synthesis procedure was adapted as follows: During the first step in the PbSe nanocrystal synthesis, i.e. the preparation of Pb-oleate precursor, the precursor was only allowed to react for ~30 minutes. Hence a small amount of acetic acid remained in the precursor mixture. The acetic acid facilitates the growth of PbSe nanostars.<sup>[1]</sup>

*PbSe rods*: rods were prepared as follows: the Pb-oleate and TOP-Se precursors were prepared as described above. 9 ml of the Pb-oleate precursor solution was injected into 13 ml DPE at 190 °C. After one minute, 0.6 ml of the TOP-Se solution was injected and the reaction was allowed to proceed for 20 minutes at a constant temperature of 140 °C. Both quenching of the reaction and purification of the NCs were performed as described above.<sup>[2]</sup>

Oriented attachment was achieved by slow evaporation of the solvent from the nanocrystal suspension placed on top of ethylene glycol as an immiscible liquid substrate, at a given temperature (called the reaction temperature). In a typical experiment, 1 mL of ethylene glycol was placed in a glass vial (Ø 10 mm). After the desired temperature (between 20 and 140 °C) was reached, 50 µL of nanocrystal suspension was injected after which the solvent was allowed to evaporate, as depicted in figure S1. The evaporation takes from 90 to 10 minutes. After evaporation a sample was taken from the ethylene glycol layer at the center of the vial and placed under vacuum to evaporate the residual ethylene glycol. All experiments were performed in a nitrogen purged glovebox.

The nanocrystals were imaged using high angle annular dark field scanning transmission electron microscopy (HAADF-STEM) performed using a double aberration corrected FEI TITAN operated at 300kV. The semi convergence angle of the electron probe used during acquisition was 21.4 mrad. The conventional TEM images were obtained with a FEI Tecnai 12.

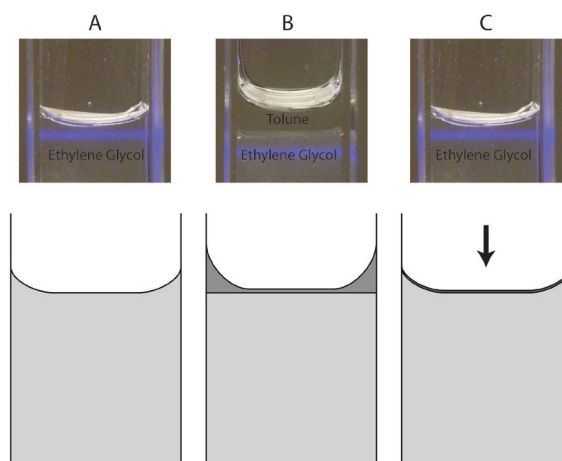


Figure S1: Cartoon of the evaporation process. Ethylene glycol is placed in a vial (A) after which the PbSe nanocrystal suspension is deposited on top of it (B). To illustrate the effect the amount of suspension has been increased tenfold in figure B. After the solvent is evaporated, a sample is taken in the centre of the vial at the air/liquid interface. The entire experiment takes place in a nitrogen purged glovebox (oxygen and water below 10 ppm).

- (1) Houtepen, A. J.; Koole, R.; Vanmaekelbergh, D.; Meeldijk, J.; Hickey, S. G. *Journal of the American Chemical Society* 2006, 128, (21), 6792-6793.
- (2) Casavola, M.; van Huis, M. A.; Bals, S.; Lambert, K.; Hens, Z.; Vanmaekelbergh, D. *Chem. Mater.* **2012**, 24 (2), 294–302.

## II Characterization of the shape and the facets of the PbSe nanocrystals by HAADF-STEM

*Nanocubes* The shape and facets of the PbSe nanocubes were investigated in detail with High Angle Annular Dark Field Scanning Transmission Electron Microscopy (HAADF-STEM). In figure S2, two HAADF-STEM images are presented, obtained from PbSe nanocrystals with a diameter of 9.9 nm. Figures S2a and S2b present images acquired with the electron beam oriented along the  $[110]$  axis and the  $[100]$  axis respectively. The edges of the projection can be identified as  $\{100\}$ ,  $\{011\}$  and  $\{111\}$  facets. Figures (c) and (d) present intensity profiles taken along the direction indicated by the arrows in (a), showing a  $\{100\} \rightarrow \{110\} \rightarrow \{100\}$  sequence of facets in (c) and a  $\{111\} \rightarrow \{110\} \rightarrow \{111\}$  sequence in (d). These results are in line with a truncated nanocube model (see inset) with 6 natural  $\{100\}$  facets and  $\{110\}$  and  $\{111\}$  truncations.

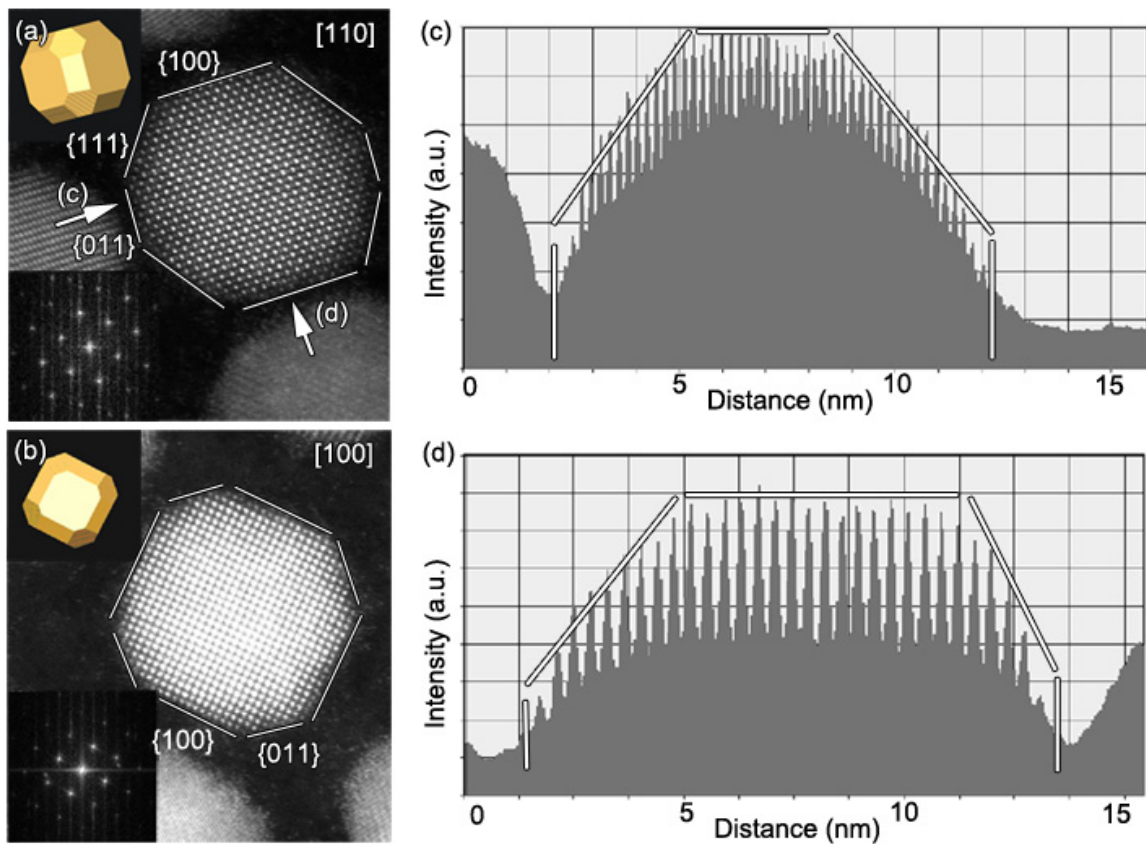
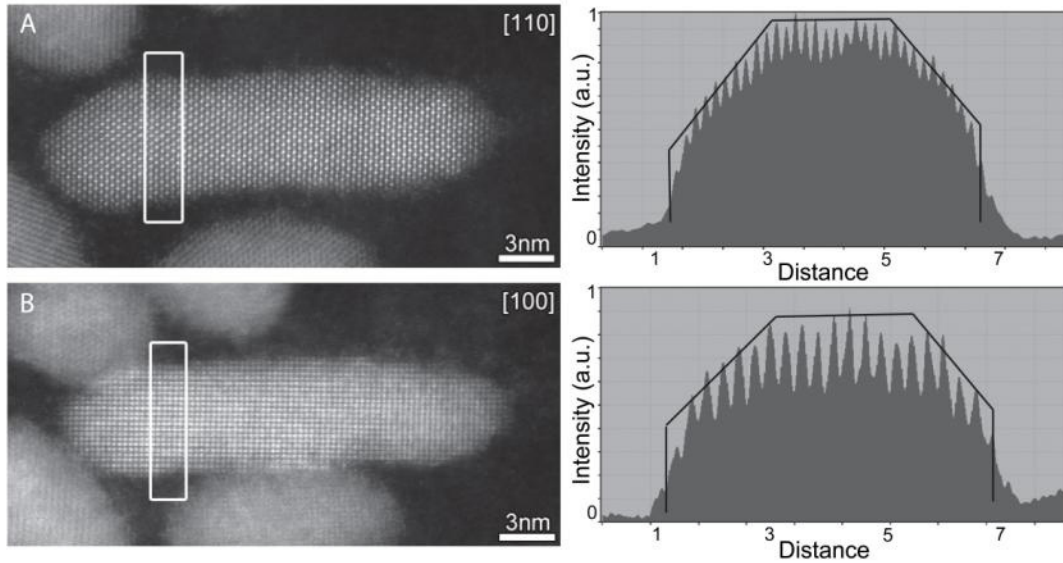


Figure S2: High resolution HAADF-STEM image of PbSe nanoparticle oriented along the  $[110]$  zone axis (a) and along the  $[100]$  zone axis (b). Both the outer shapes of the 2-D projection images and the intensity profiles (c,d) corresponds to our model of a cube with truncated  $\{110\}$  and  $\{111\}$  facets.

*Nanorods* A similar study was performed for PbSe nanorods as shown in figure S3. It was found that the tips of the nanorods yield a smooth  $\{100\}$  termination whereas the long facets are roughened  $\{100\}$  and  $\{110\}$  facets.



*Figure S3: High resolution HAADF-STEM image of PbSe nanorod oriented along the [110] zone axis (a) and along the [100] zone axis (b). Both the outer shapes of the projection and the intensity profiles corresponds to our model of a nanorod with truncated  $\{100\}$  and  $\{110\}$  facets along the long facets and  $\{100\}$  termination along the short facets.*

### III Effect of the crystal size on the attachment of PbSe nanocubes.

Various sizes of PbSe truncated nanocubes have been used in order to study the size dependence of the oriented attachment. In figures S4-S6 the structures obtained with three different sizes of PbSe NCs, with a diameter of 4.4, 7.5 and 9.9 nm, are presented. In all cases, oriented attachment leads to linear 1-D or 2-D cubic structures. However, the smallest NCs are much more reactive and show oriented attachment already at room temperature, while the 9.9 nm particles show oriented attachment at and above 100 °C only.

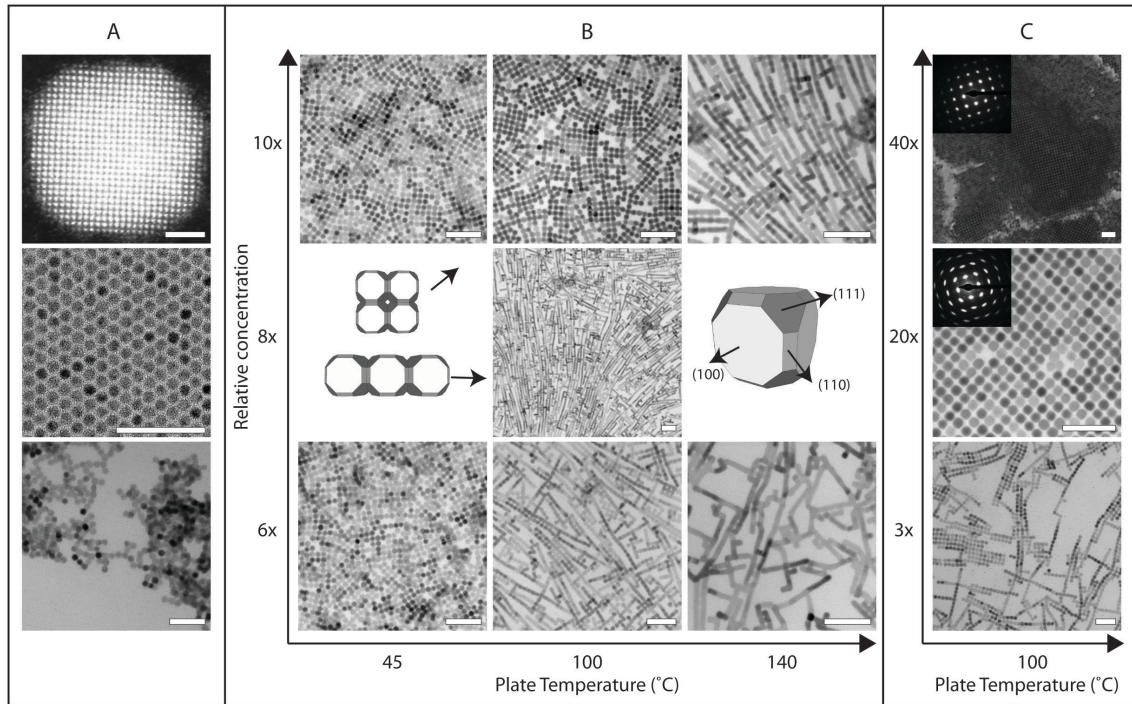


Figure S4: Overview of the obtained structures. Panel A from top to bottom; Top; 9.9 nm NC showing the truncation along the  $\{110\}$  planes. Middle; Hexagonal ordering of 7.0 nm PbSe|CdSe core shell structures on ethylene glycol at 100 °C. The CdSe acts as protection, hence no oriented attachment is observed. Bottom; Aggregates of 7.5 nm NC observed when low concentrations were used ( $<2x C_{Ref} = 140$  nM for the 7.5 nm particles). Panel B: PbSe NCs with a diameter of 7.5 nm, Panel C: PbSe NCs with a diameter of 9.9 nm. From bottom to top increasing particle concentration with respect to the lowest concentration used. The complete data set can be found in figure S5 and S6. From left to right, for panel B, increasing temperature of the reaction. At low concentrations predominately linear aggregation with two bonding sites is observed. With increasing concentration cubic ordering occurs with oriented attachment that involves 4 bonding sites. By increasing the temperature of the reaction the reversed trend can be observed, at low temperature cubic arrangement occurs while at high temperature linear attachment is predominant. From the electron diffractogram in the inset in the 2-D and 3-D structures in panel C it can be concluded that the particles are not only oriented on the NC scale but also on the atomic scale. The scale bar in the top image of panel A represents 2 nm, all other scale bars represent 50 nm.

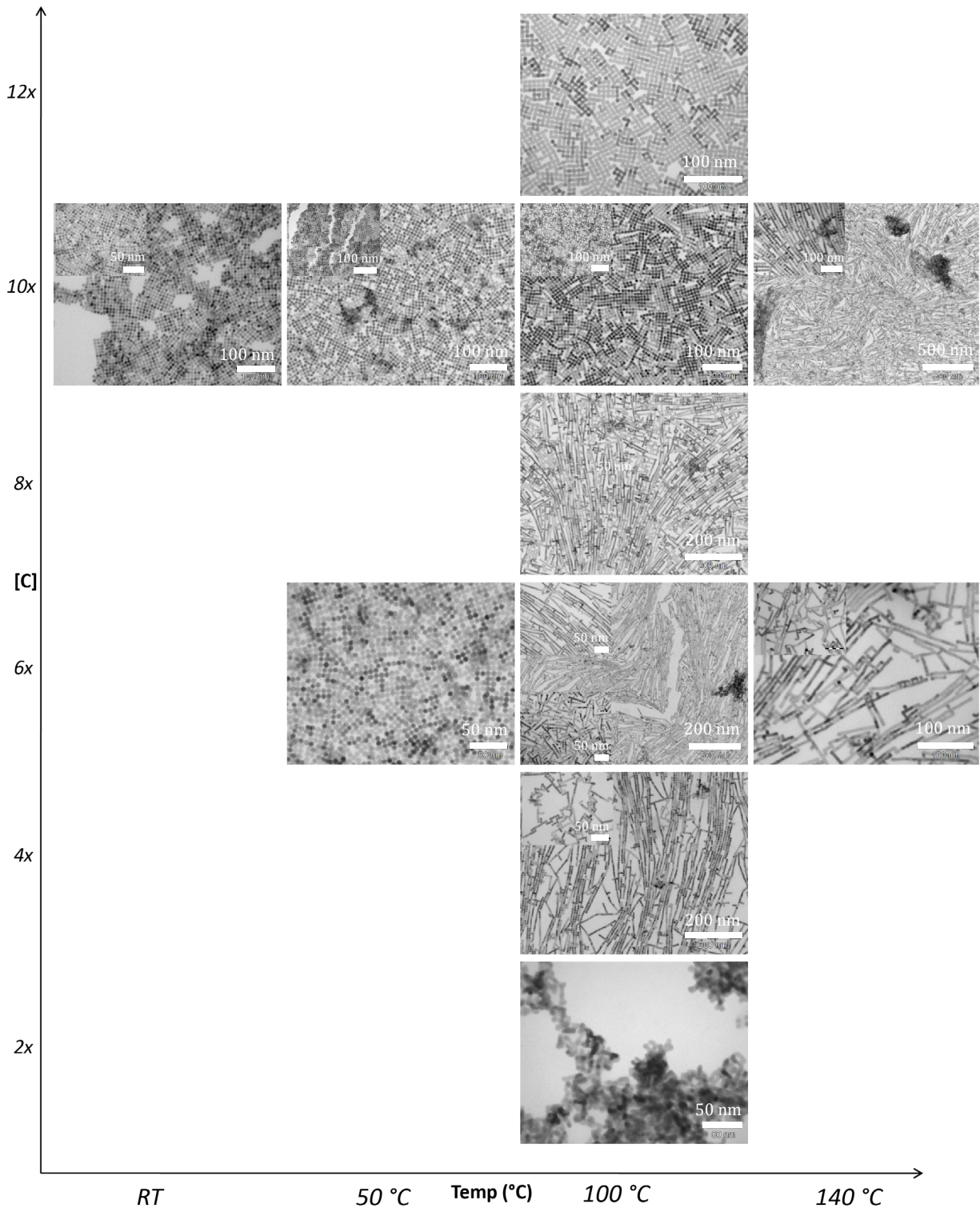


Figure S5: Oriented attachment of 7.5 nm PbSe in toluene casted on ethylene glycol at various temperatures using also different NC concentrations relative to the lowest concentration.

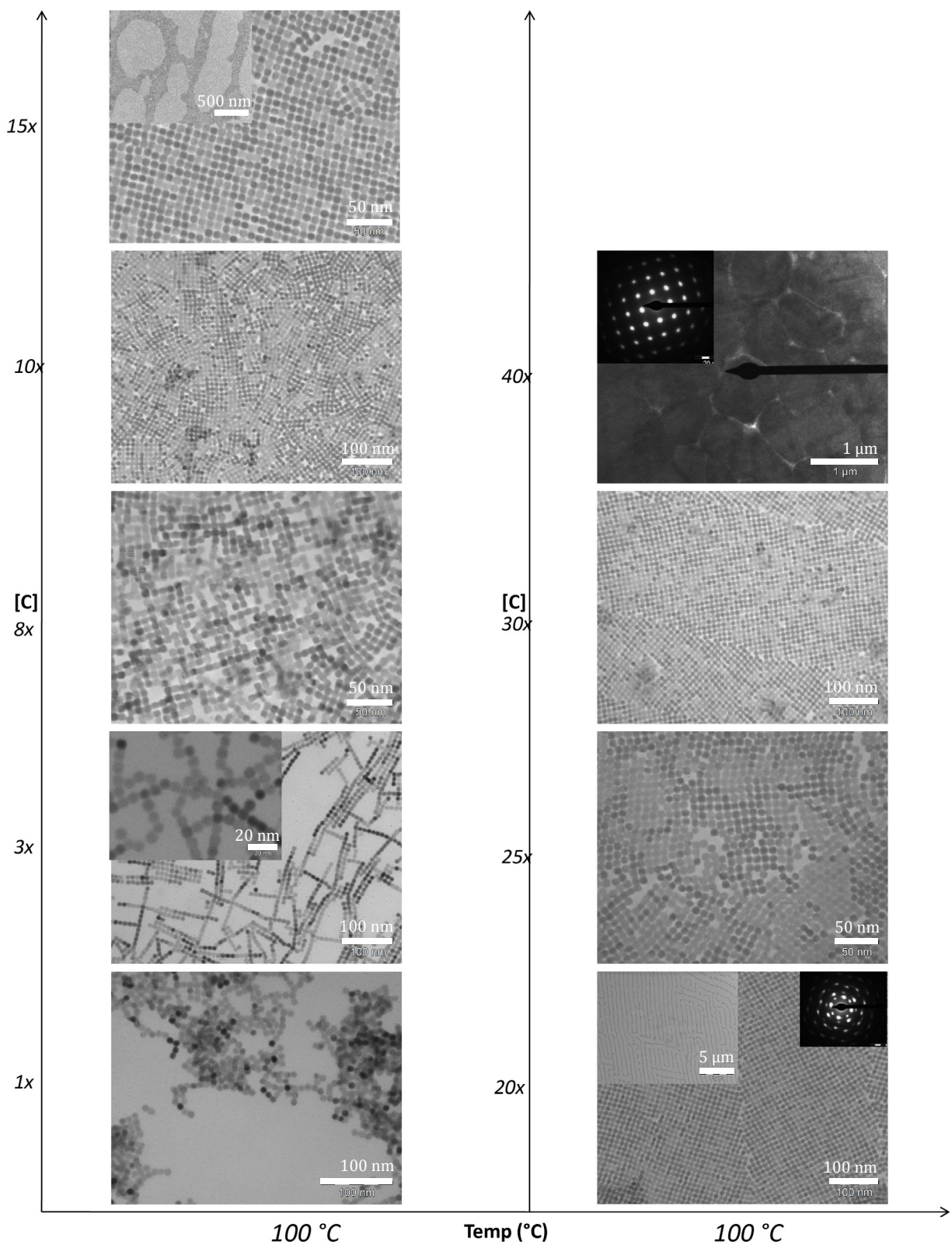


Figure S6: Oriented attachment of 9.9 nm PbSe NCs in toluene on ethylene glycol at 100 °C, using different NC concentrations relative to the lowest concentration.

#### IV Overview of the structures formed by oriented attachment in a hexane dispersion

Figure S7 presents results of experiments using PbSe NC dispersions with hexane as a solvent instead of toluene. Oriented attachment leads to the formation of 1-D wires and 2-D sheets in a similar way as with toluene as a solvent. However, with hexane as solvent, there is a tendency to form more extended cubic sheets. In addition, oriented attachment sets on at a lower temperature.

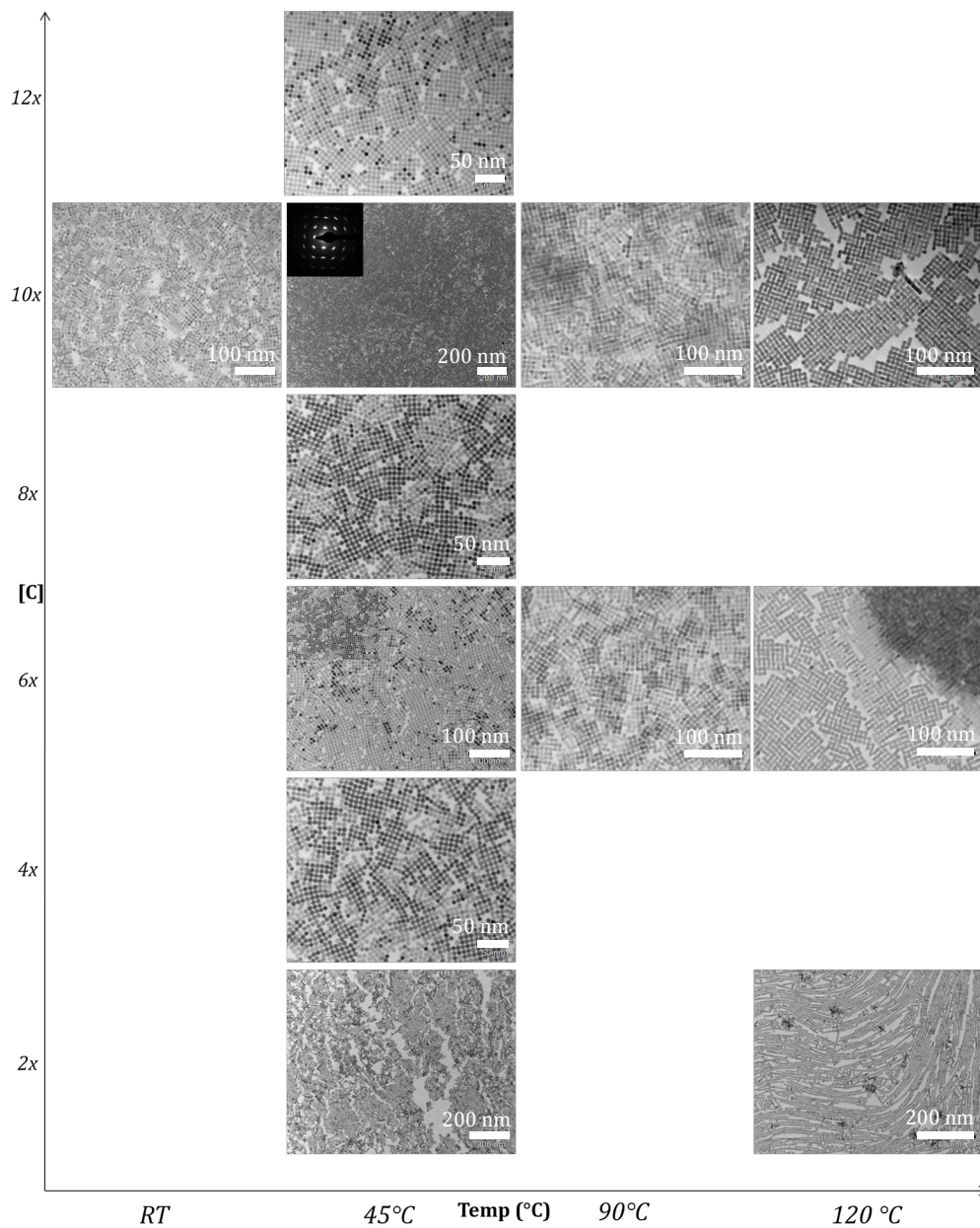


Figure S7: Oriented attachment of 7.5 nm PbSe NCs on ethylene glycol using hexane as solvent, at various temperatures and with different concentrations relative to the lowest concentration.

## V Effect of addition of oleic acid capping molecules to the ethylene glycol

The effect of oleic acid capping ligands added to the glycol phase, for different concentrations of the nanocrystals, is presented in figure S8. We used 5.4 nm PbSe nanocrystals. 50  $\mu\text{L}$  of the nanocrystal suspension was injected in a 78.5  $\text{mm}^2$  reaction vessel containing 1 mL ethylene glycol. If no capping was added, it can be observed that for this size nanocrystals a honeycomb type-structure exist at a concentration of  $\sim 11\text{-}20$  mol/L. The honeycomb structure is always in equilibrium with the rod-like structures. When additional capping ligands were added oriented attachment is not observed, typical hexagonal self-assembly is achieved instead. When even more ligands were added large crystallites were observed as is shown in the insets. The same trend was observed when n-tetradecyl phosphonic acid or octadecyl phosphonic acid was used as additional capping ligands (see figure S9)

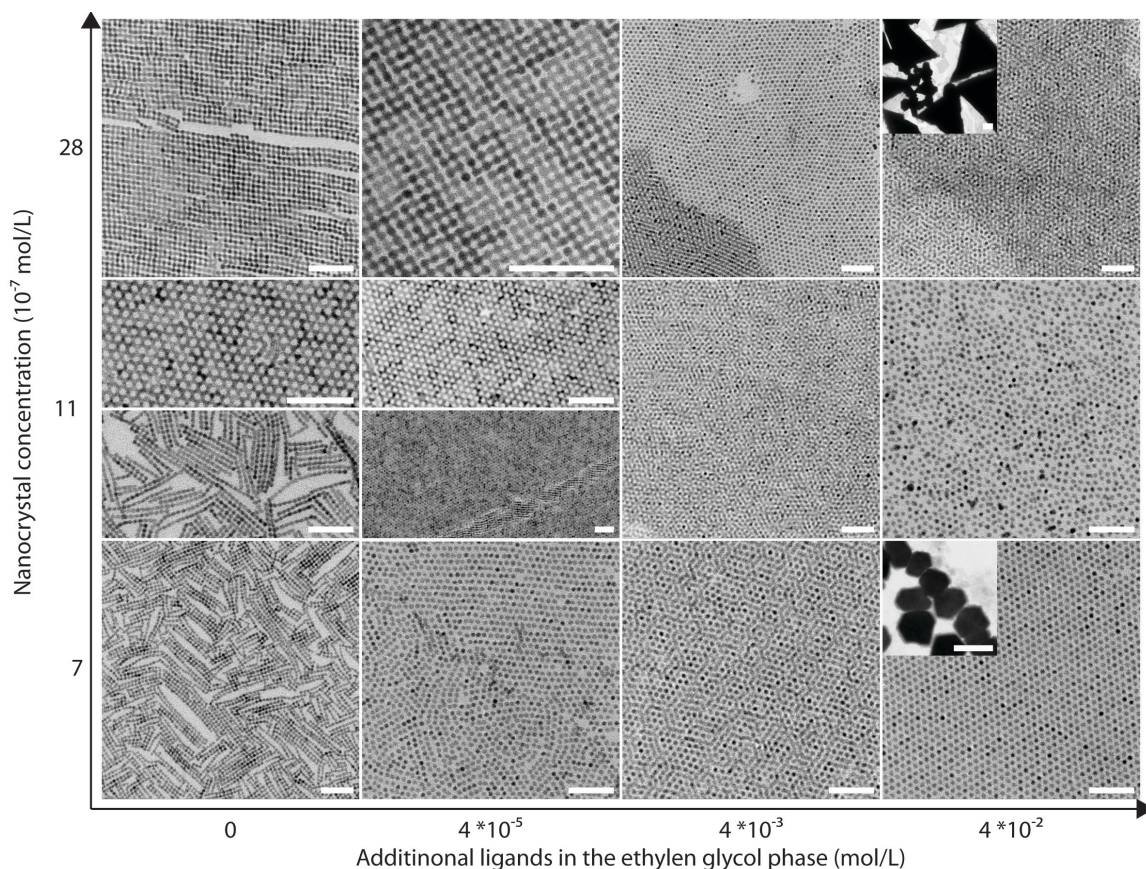
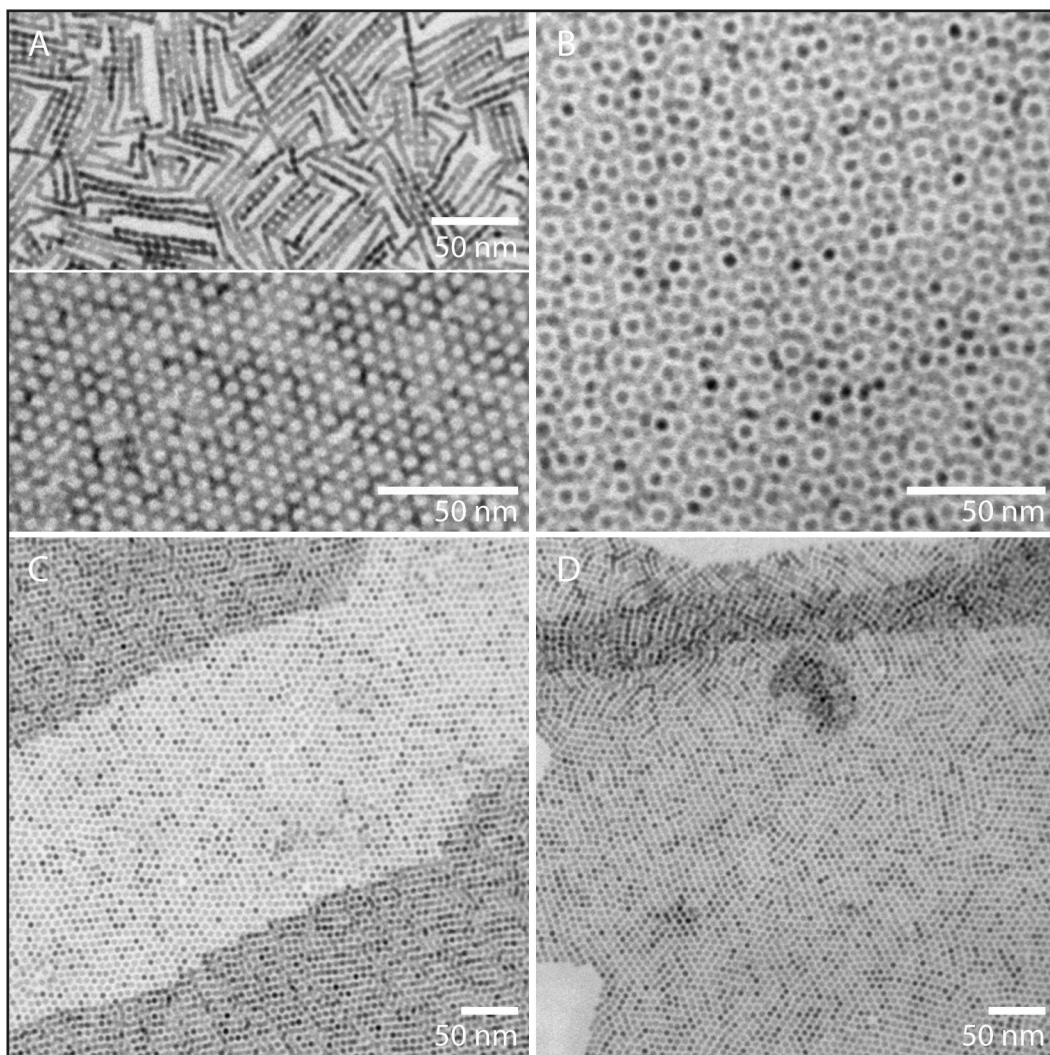


Figure S8: Effect of additional oleic acid capping ligands in the glycol phase as function of the nanocrystal concentration for 5.4 nm PbSe nanocrystals. The scale bars represent 50 nm except for the insets where they represent 1  $\mu\text{m}$ .



*Figure S9: Effect of various capping ligands to the ethylene glycol phase. A) no additional ligands. B) Addition of  $4 \cdot 10^{-4}$  mol/L oleic acid. C) Addition of  $4 \cdot 10^{-4}$  mol/L n-tetradecyl phosphoric acid. D) Addition of  $4 \cdot 10^{-4}$  mol/L octadecyl phosphoric acid.*

## VI HAADF-STEM study of defects in oriented attachment

The irreversible strong bonding of the nanocrystals by oriented attachment leads inherently to imperfect attachment events. Imperfect attachment induces crystal defects during the growth<sup>[3]</sup>. In the case reported here, oriented attachment does not always occur by connection of two perfectly aligned {100} facets. Figure S10A shows two attached nanocubes, their opposed {100} planes were, however, not completely parallel resulting in an edge dislocation. Figure S10B shows another defective way of attachment: the nanocubes in the linear structure have parallel {100} bonding facets; they are, however, all differently rotated in the plane perpendicular to the bond axis.

When the structures formed by oriented attachment were thermally treated under nitrogen, remarkable atomic reconfigurations were observed in which the effects of misorientations were annealed, and the original shape of the building blocks is gradually washed out. A part of a nearly perfectly smooth PbSe sheet obtained by oriented attachment and thermal annealing is presented in Figure S10C; only a small trace of the early connection of two nanocrystals is still visible. The results of oriented attachment of small PbSe nanocubes at 50 °C, and further annealing are presented in Fig. S11. Panel A shows a planar sheet formed by oriented attachment of PbSe nanocubes 5.4 nm in diameter; the structure that constitutes an atomic PbSe rocksalt single crystal still shows the signature of the original building blocks. If oriented attachment is followed by a thermal treatment at 80 °C, a further atomic smoothing is observed leading to a two-dimensional network in which the original nanocubes can no longer be recognized.

(3) Penn, R. L.; Banfield, J. F. *Science* **1998**, 281, (5379), 969-971.

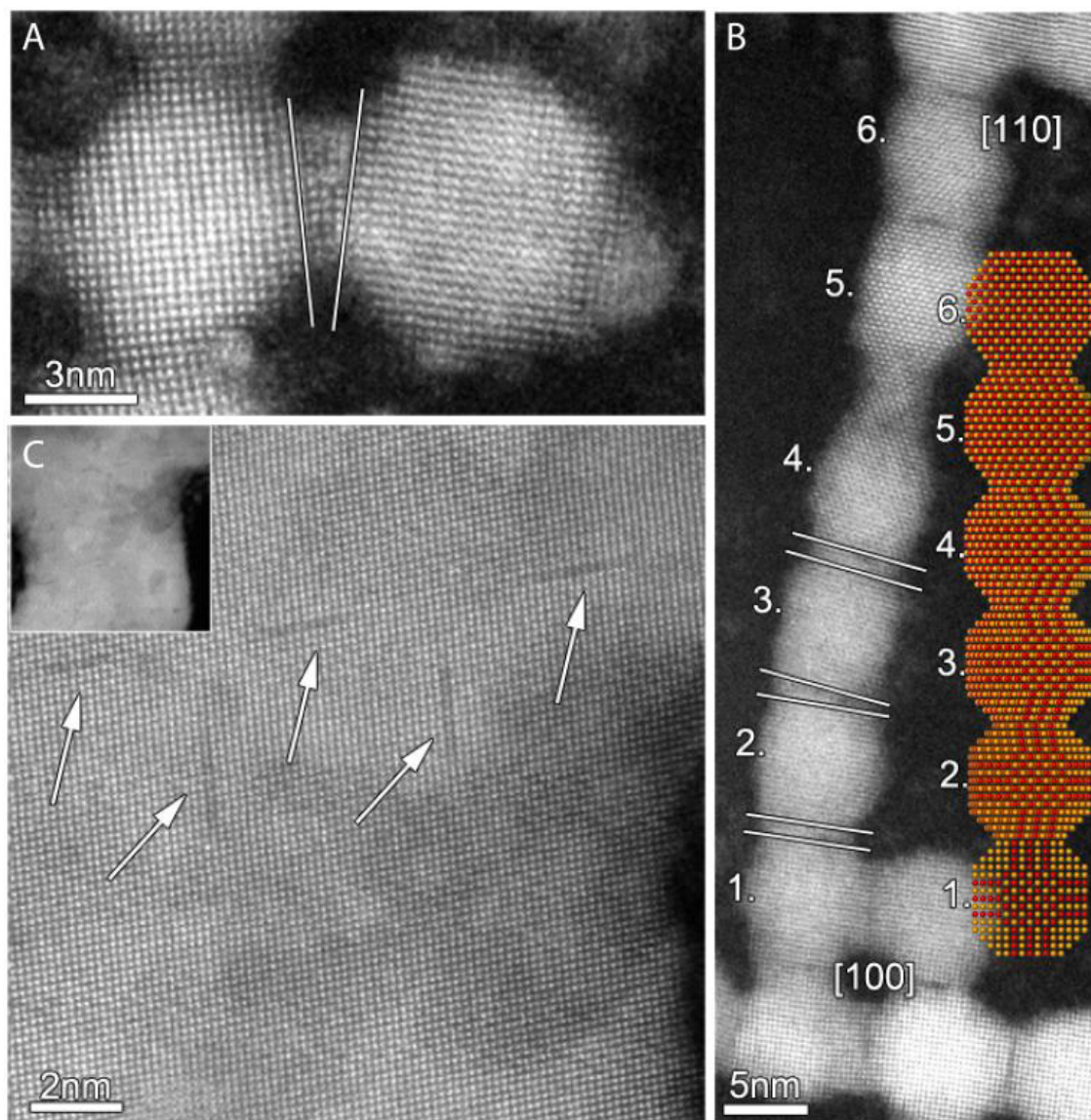


Figure S10: Imperfect oriented attachment of PbSe nanocrystals. A) Two attached NC with their  $\{100\}$  planes being not completely parallel, resulting in an edge dislocation. B) The NCs are rotated over  $45^\circ$  over 6 particles in respect to the bonding axis, resulting in a screw dislocation. C) Nearly defect free single-crystalline sheet with a nearly homogenous thickness and lateral dimensions in the  $\mu\text{m}$  range. The arrow indicates missing rows where the original particles were situated. The particles used in A and B were 7.5 nm PbSe NCs while in C 9.9 nm PbSe NCs were used.

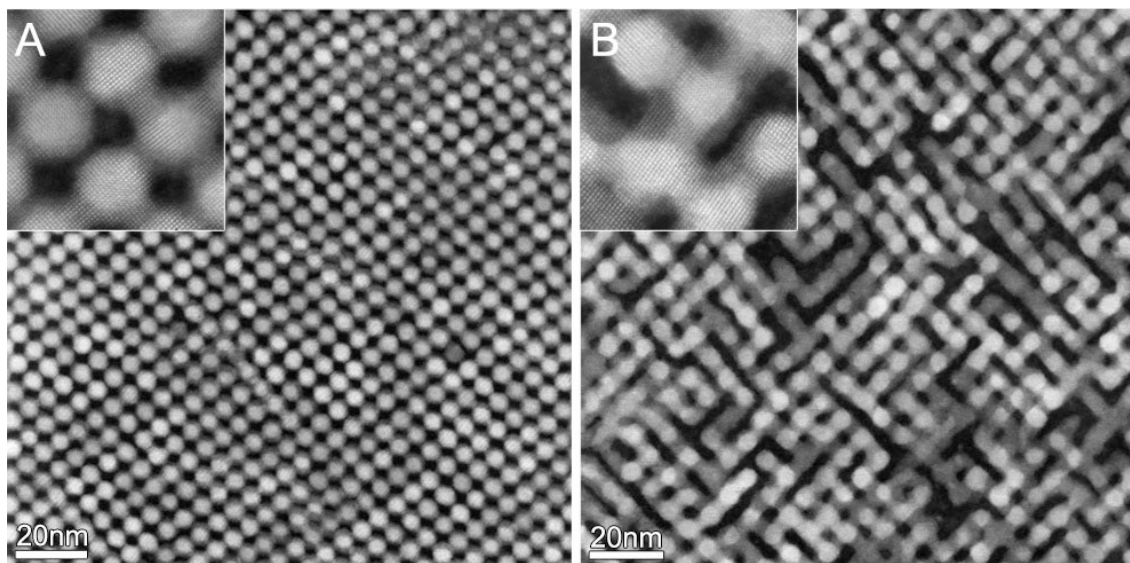


Figure S11: The fusing process of 5.4nm PbSe nanocrystals. Both samples were similarly grown at 50 °C for which a single crystalline square lattice was obtained as given in figure A. After evaporation the temperature was increased to 80 °C for figure B.

## VII Oriented attachment of PbSe rods and stars

*PbSe rods* Besides the oriented attachment of truncated cubic PbSe NCs, we also studied the oriented attachment of PbSe nanorods and nanostars. The rods have smooth  $\{100\}$  facets on both the tips; the long-side facets also correspond to  $\{100\}$ , but there is considerable roughening. Figure S12 shows a sample before and after attachment took place. It is evident that the rods only attach with the  $\{100\}$  tip facets forming strings of rods, and that the rough side-facets are not used in the attachment. This is possibly caused by the roughening of these facets that also could lead to a stronger absorption of the surfactant molecules. The formation of exclusively 1-D structures was observed in broad range of temperature and concentration.

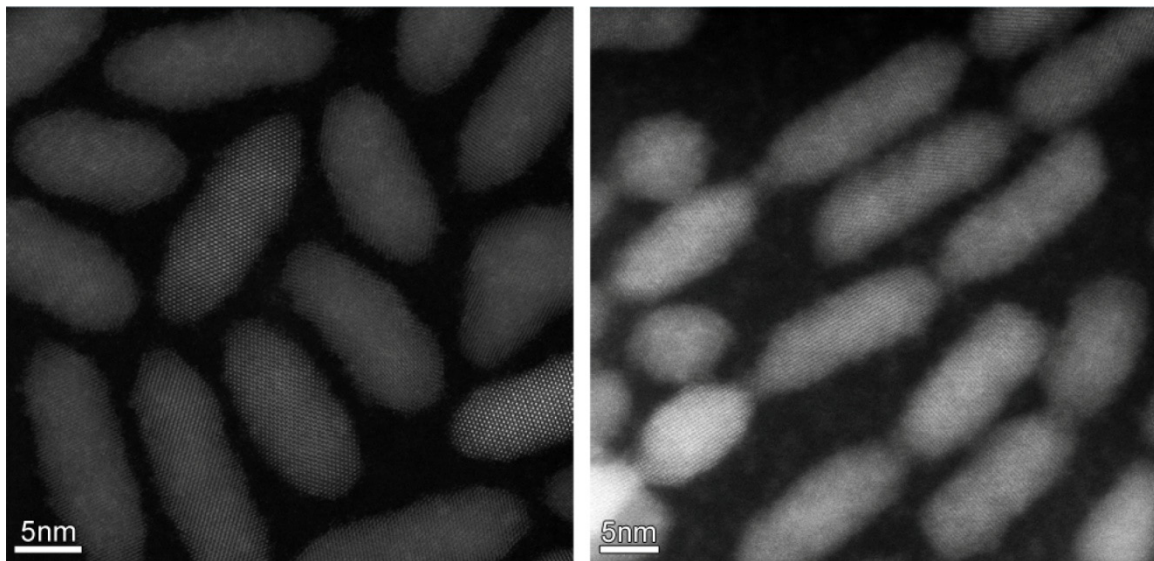


Figure S12: Linear oriented attachment of PbSe nanorods. Left: drop casted nanorods, and right a picture after solvent evaporation at a temperature of 20 °C, leading to attachment via the  $\{100\}$  tips.

*PbSe stars* Nanostars were synthesised as in Ref. 1, and used in experiments of oriented attachment. These stars have 8 tips that presumably end as very small {100} facets. Oriented attachment of PbSe nanostars resulted in cubic- and wire-like arrangement of the stars, depending on the growth temperature. As can be seen in figure S13, individual PbSe stars are usually ‘lying’ on a side. A temperature increase led to oriented attachment, resulting in a cubic architecture, which was, however, less ordered than in the case of nanocubes. In these square architectures, the stars stand upright and were exclusively connected via their tips, presumably being small {100} end-facets. When a higher temperature was used for solvent evaporation, more wire-like structures are observed, in a similar way for the truncated cubes (see figure S13 and S14).

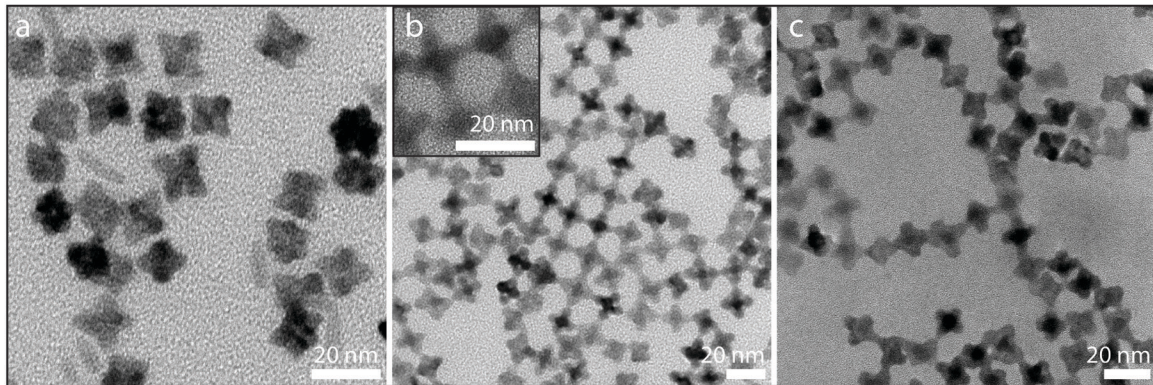


Figure S13: TEM study on the oriented attachment of PbSe nanostars. a, drop casted sample. b, oriented attachment grown at 100 °C. c, oriented attachment grown at 150 °C.

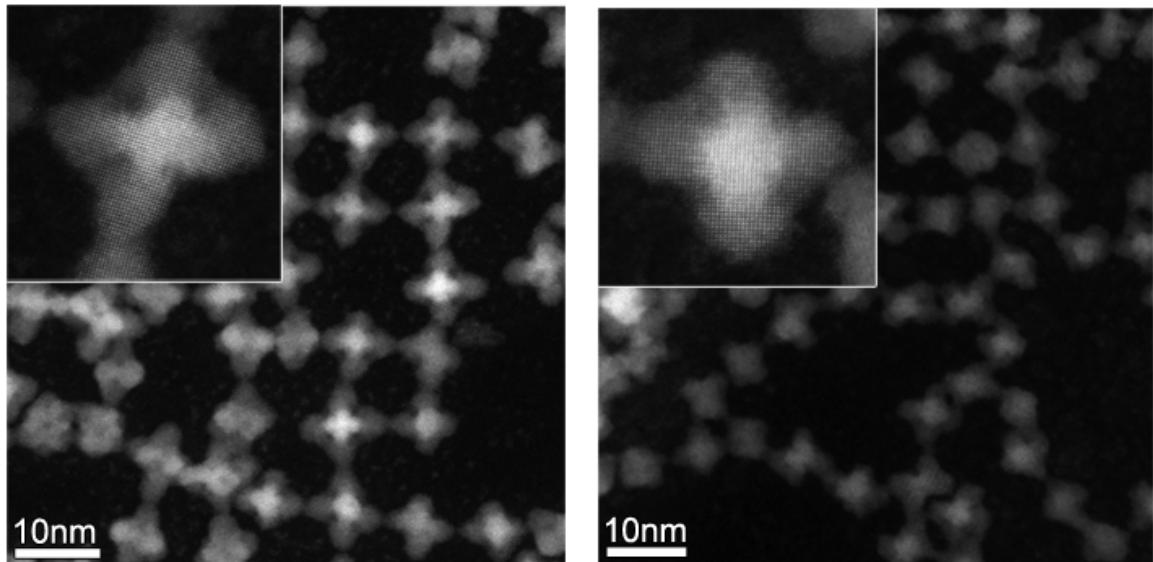


Figure S14: In-depth HAADF-STEM study on the oriented attachment of PbSe nanostars. Left a sample grown at 100 °C and right a sample grown at 150 °C.

## VIII Conversion of PbSe sheets to CdSe or Cu<sub>2-x</sub>Se sheets by ion exchange

The conversion of a PbSe sheet into a CdSe sheet was obtained by placing the PbSe sheet on a substrate (TEM-grid or silicon (100) wafer), which was then brought in contact with a 0.1 M Cd-oleate solution in 1-octadecene and heated up to 130 °C for 2 hours. The results presented in figure S15 provide evidence that the sheets preserve their cubic particle symmetry, while from the electron diffraction patterns and SEM-EDX results it follows that the atomic lattice was changed completely from rocksalt to zinc blende. SEM-EDX spectra show that the sheets are transformed from a PbSe to a CdSe composition. The electron diffraction pattern of the CdSe sheets corresponds with zinc blende CdSe with unit cell vectors ( $a=b=c$ ) of 5.873 nm<sup>[4]</sup> instead of the typical 6.050 nm<sup>[5]</sup>. Note that zinc blende CdSe with these parameters were also reported in the literature<sup>[6]</sup>. In the tables given with the radial intensity plots of the diffraction patterns (middle of figure S15), the measured values are compared with the values from literature. A good agreement can be observed for both the PbSe and the CdSe values. Strikingly, one diffraction peak of the CdSe sheets could not be fitted, and its origin remains unclear thus far.

The conversion of PbSe sheets into Cu<sub>2-x</sub>Se was obtained by first converting the PbSe sheet to a CdSe sheet as described above.<sup>[7]</sup> After the CdSe exchange the TEM grids were placed in a 2 mL 0.03M solution of tetrakis(acetonitrile)copper(I) hexafluorophosphate in methanol for 1 min, after which they were rinsed with toluene and methanol. The results in figure S16 provide evidence that the sheets preserved their cubic particle symmetry, while from the TEM-EDX results it follows that the atomic lattice is changed to Cu<sub>2-x</sub>Se.

(4). JCPDS-ICCD, **2010**, card no. 04-012-6324

(5). JCPDS-ICCD, **2010**, card no. 01-073-6987

(6). JCPDS-ICCD, **2010**, card no. 00-006-0354

(7). P. K. Jain, L. Amirav, S. Aloni, A. P. Alivisatos, *Journal of the American Chemical Society* **2010**, 132, 9997.

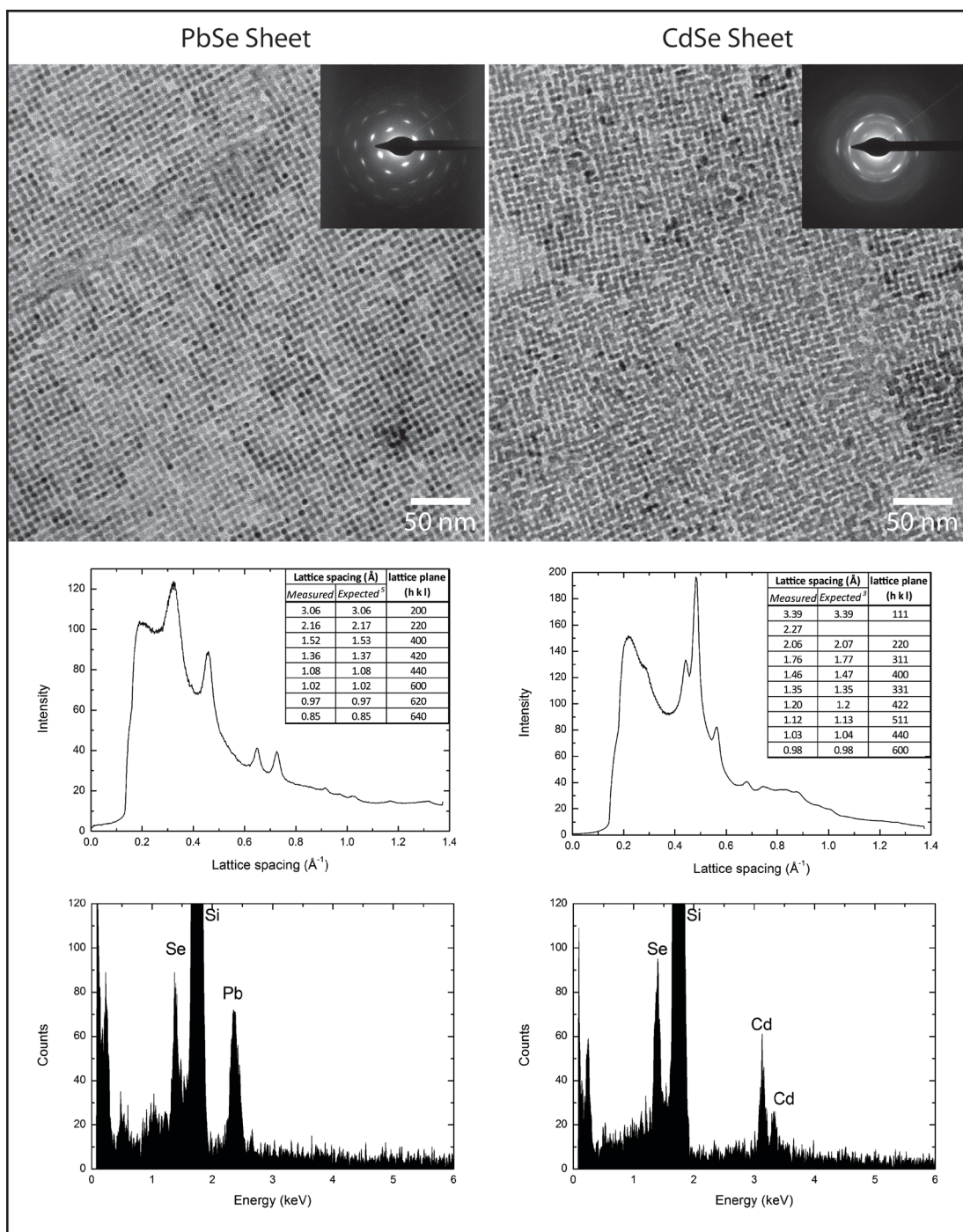


Figure S15: TEM-images, electron diffractograms and EDX measurements of a PbSe sheet, and a CdSe sheet resulting from a Cd-for-Pb cation exchange reaction starting from a PbSe sheet. From top to bottom: TEM-images, radial intensity plots of the electron diffraction patterns given in the insets, and the corresponding values for the measurement and literature, and SEM-EDX measurements of a comparable sample in a SEM.

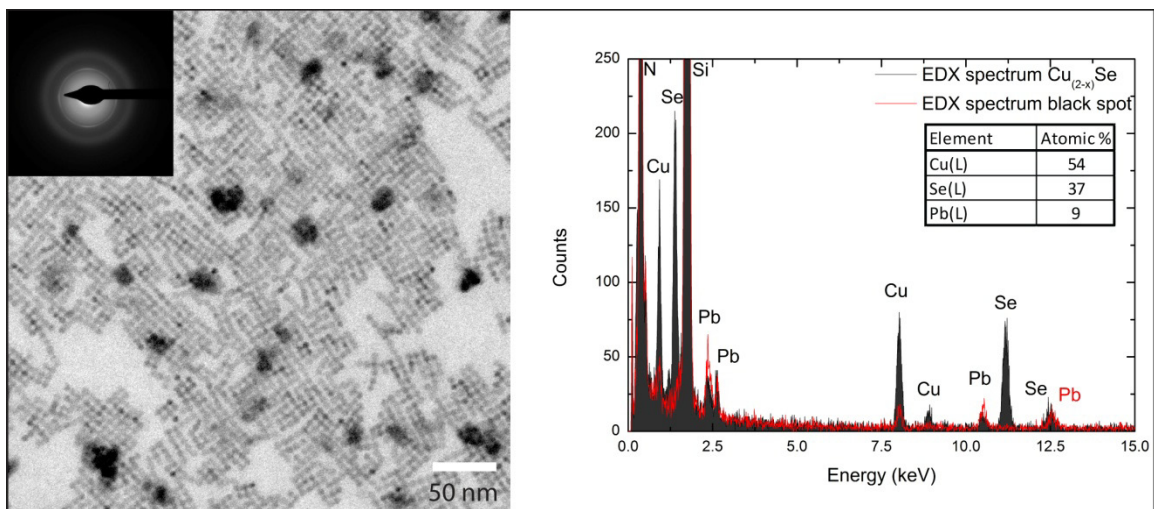


Figure S16: TEM image and TEM-EDX spectrum of the obtained structure after cation exchange with  $\text{Cu}^+$ . The EDX spectrum of the NC (black) shows both Cu, Se and some residual Pb ions while the black spots in the TEM image are composed out of Pb and Cu.

## IX XRD analysis of the structures formed by oriented attachment

In figure S17 we present XRD results of the 2-D structures formed by oriented attachment compared to those of individual unreacted nanocrystals. The wavelength used for the XRD measurements was  $1.54 \text{ \AA}$  and the spot size was approximately  $25 \text{ mm}^2$ . For the drop-casted unreacted sample, the diffraction peaks of several planar facets can be observed i.e. the NCs are randomly oriented on the substrate. The sample after oriented attachment shows mainly the (200) and to a smaller extent the (220) peaks. This indicates that in the reacted structure nearly all  $\{100\}$  facets are perpendicular to the surface, in agreement with 2-D attachment via the four upstanding  $\{100\}$  facets.

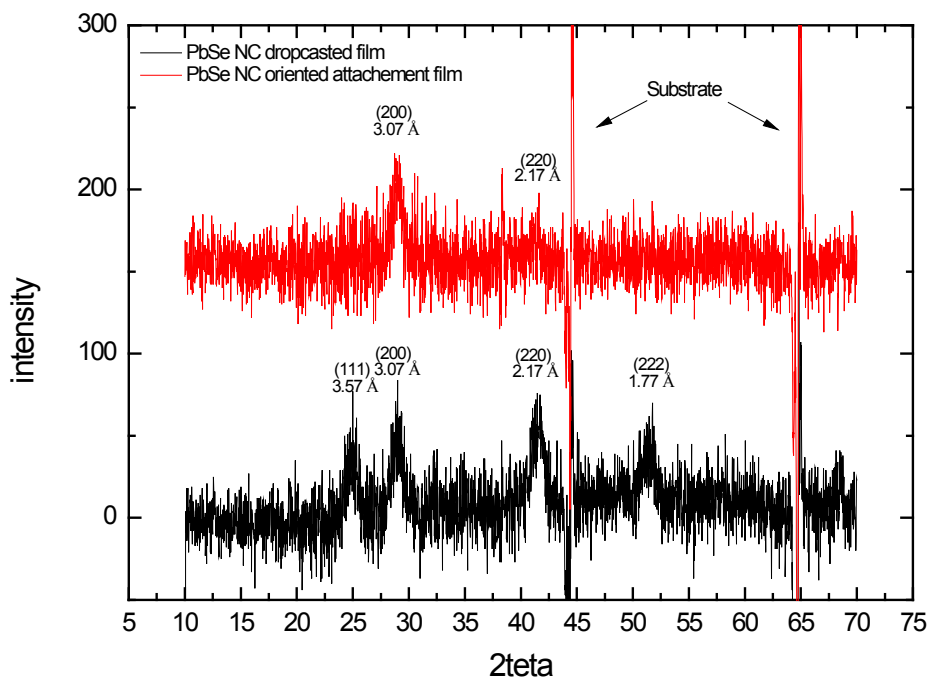


Figure S17: XRD pattern of truncated nanocubes that are drop-casted (black), and after solvent evaporation at elevated temperature leading to oriented attachment (red). The drop casted sample clearly shows several diffraction peaks due to different orientations of the NCs on the substrate, while the oriented film mainly shows the diffraction peaks of the (200) planes, showing preferential orientation of the cubes in the 2-D sheets.

## X GISAXS study of the oriented attachment in the glycol-ethylene/suspension reactor system

In-situ GISAXS measurements have been performed to study the assembly process in more detail. The measurements were carried out in the synchrotron center in Grenoble at beamline ID10 under experiment SC-3300. During and after the evaporation of the toluene, GISAXS measurements were performed with the x-ray spot probing the liquid-air interface. In figure S16 an example of a GISAXS pattern after evaporation of the solvent is presented. Diffraction peaks at a  $Q$  value of  $0.624 \text{ nm}^{-1}$  indicate ordered domains of the PbSe  $9.9 \text{ nm}$  cubes on the glycol; the average inter-particle distance is measured to be  $10.1 \text{ nm}$ , indicating that ligand-free facets are attached.

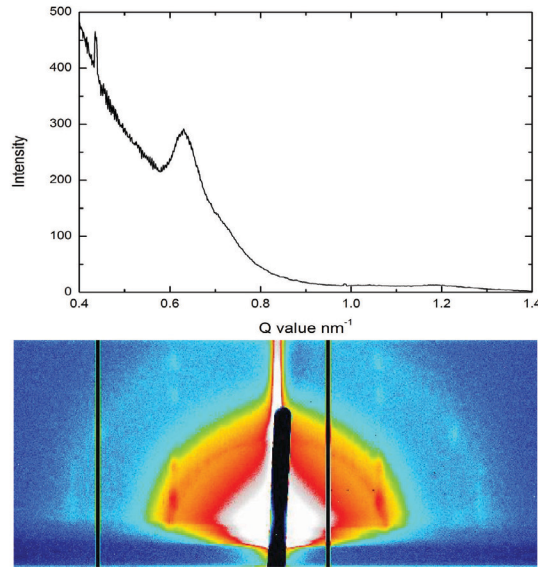


Figure S18: In-situ GISAXS pattern and corresponding intensity vs. wave-vector graph of a structure formed of  $9.9 \text{ nm}$  PbSe NCs after complete evaporation of the solvent. From the graph a dominant peak at a  $Q$ -value of  $0.64 \text{ nm}^{-1}$  can be observed.